PHYSICAL REVIEW D **86,** 076016 (2012)

Incorporating fermions in the Gaussian effective potential: The Higgs-top sector

Fabio Siringo

Dipartimento di Fisica e Astronomia dell'Università di Catania, INFN Sezione di Catania, Via Santa Sofia 64, I-95123 Catania, Italy

(Received 15 August 2012; published 31 October 2012)

The Higgs-top model is studied by a nonperturbative variational extension of the Gaussian effective potential that incorporates fermions. In the limit of a very strong Yukawa coupling the one-loop result is shown to follow a single-parameter scaling while the Gaussian fluctuations give rise to important deviations from scaling and to a reduction of the vacuum expectation value and of the top mass. A good general agreement is found with lattice data when a comparison can be made. The vacuum is shown to be stable for any choice of the Yukawa coupling, at variance with renormalized perturbation theory. Analytical results are provided for a few observables like the renormalized mass of the Higgs boson and its wave function renormalization constant. Extensions to gauge theories like QCD are briefly discussed.

DOI: 10.1103/PhysRevD.86.076016 PACS numbers: 11.15.Tk, 14.80.Bn, 12.15.Ff

I. INTRODUCTION

Above the QCD scale, when all the couplings are small enough, the Standard Model (SM) of the fundamental interactions can be studied by perturbation theory. However, there are energy ranges and sectors of the SM where nonperturbative methods are welcome for comparison and control of the perturbative approximation, for instance, when the QCD becomes strongly coupled, or in the hypothesis of a large Higgs mass and a strong self-coupling of the Higgs sector, that has been almost ruled out by experiments. Another interesting system is the Higgs-top sector, where nonperturbative effects could be found because the Yukawa interaction $y \approx 0.7$ is not as small as other fermions.

The most widely used nonperturbative approach is the numerical simulation on a finite lattice, which allows for an exact treatment of the Lagrangian but is plagued by many shortcomings like the small size of the sample, border effects, the lack of any analytical result, and some specific problems about incorporating fermions [1–6]. For instance, a duplication problem does not allow a simple description of a model with an odd number of fermions or even only one fermion [7]. Moreover, the finite lattice spacing is equivalent to the existence of a finite energy cutoff that cannot be removed.

This last point does not seem to be an important issue any more, since our modern understanding is that the SM must be considered an effective model holding up to a finite energy scale. The triviality of the scalar theory requires that a finite cutoff should be present in the model, and even a large cutoff can be simulated on the lattice if the sample size is large enough and allows for long correlation lengths compared to the lattice spacing. On the other hand, the existence of a finite cutoff has opened the way to a class of variational approximations, since their typical UV problems are cured by the existence of a limited energy range. The Gaussian effective potential (GEP) [8–11] is a variational tool that has been recently shown to provide a very good agreement with lattice data whenever a finite cutoff is used in the analytical derivation [12]. The GEP is not exact but is based on a nonperturbative approximation, and its predictions are expected to hold even when perturbation theory breaks down. Moreover the GEP yields simple analytical results and has been recently shown to shed some light on the physics of several systems ranging from superconductors [13,14] to magnetic systems [15] to non-Abelian gauge theories [16] and the Higgs sector of the SM [12,17–19].

It would be interesting to extend the GEP to the Higgs-top sector of the SM, which would require the inclusion of fermions in the derivation of the effective potential. The problem is of some interest by itself because of the failure of incorporating fermions, which was reported in the past. In fact, a direct attempt to include fermions was shown to give a result that is equivalent to the perturbative one-loop fermionic term of the effective potential [20]. Thus for fermions the GEP has always been regarded as useless. Quite recently an hybrid method has been proposed for incorporating fermions in the GEP [15]: the technique has been tested in the framework of the well-studied two-dimensional Hubbard Hamiltonian at half filling, describing a gas of interacting fermions in the antiferromagnetic phase. The method predicts the exact magnetization in the strong coupling limit, and for large couplings it improves over other approximations like RPA, in close agreement with lattice data. Instead of attempting to evaluate the GEP directly, in this method the fermions are integrated exactly, and the resulting effective Lagrangian is expanded in powers of the scalar field. Then the GEP is evaluated by the usual variational method. In the strong coupling limit the second order term of the expansion has been shown to be enough for an accurate description of the fermionic fluctuations that are included at the Gaussian level [15].

In this paper the same hybrid technique is used for incorporating fermions in a self-consistent variational approach to the Higgs-top model, a toy model containing a self-interacting scalar particle interacting with a massless fermion through a standard Yukawa interaction. In this model, that mimics the mechanism of mass generation of the SM, the symmetry breaking is driven by the Yuakawa interaction, and even when the classical scalar potential does not show any symmetry breaking, the effective potential can have a minimum with a nonvanishing vacuum expectation value (vev) of the scalar field. Thus while the fermions acquire a mass through the Yukawa interaction, it is the fermion that drives the symmetry breaking determining the vev. A naive discussion of symmetry breaking, based on the classical potential, does not work in the present model where the vev must be determined by the full self-consistent quantum effective potential.

In the next sections the GEP is evaluated for the Higgs-top model, and the result is compared with available lattice simulation data [21] and with the standard one-loop approximation. A full agreement is found with the lattice data when a comparison can be made. Moreover the method is almost analytical, and explicit analytical results can be obtained for the pole of the scalar propagator, the wave function renormalization constant, and other relevant observables. For instance, by inspection of the analytical expression of the effective potential, the vacuum can be shown to be stable for any choice of the bare parameters, at variance with renormalized perturbation theory. The method is nonperturbative, and deviations from the one-loop approximation can be regarded as a measure of nonperturbative effects that are shown to be large in the strong coupling limit.

Besides the physical relevance of the present model, the problem of incorporating fermions in a nonperturbative method is by itself relevant because of the possible extension to non-Abelian strongly interacting theories like QCD. For instance the GEP has been evaluated for the pure SU(2) theory [16] but no previous attempts of incorporating fermions have been reported. The present method could be explored in that context.

The paper is organized as follows: in Sec. II the method is described in detail; in Sec. III the GEP is compared with lattice data; in Sec. IV the strong coupling limit is explored and compared with the one-loop result; and some final remarks and directions for future work are reported in Sec. V.

II. GEP IN THE HIGGS-TOP MODEL

In the Euclidean formalism the Higgs-top model is described by the Lagrangian

$$\mathcal{L} = \mathcal{L}_\phi + \mathcal{L}_t + \mathcal{L}_y, \tag{1}$$

where $\mathcal{L}_\phi$ is the Lagrangian of a self-interacting scalar field ϕ

$$\mathcal{L}_\phi = \frac{1}{2}\partial^\mu\phi\partial_\mu\phi + V_c(\phi), \tag{2}$$

with a classical potential

$$V_c(\phi) = \frac{1}{2}m_B^2\phi^2 + \frac{1}{4!}\lambda_B\phi^4. \tag{3}$$

$\mathcal{L}_t$ is the Lagrangian for a set of N_f massless free Fermi fields ψ_j

$$\mathcal{L}_t = -i\sum_{j=1}^{N_f}\bar{\psi}_j\gamma^\mu\partial_\mu\psi_j, \tag{4}$$

and $\mathcal{L}_y$ contains a set of Yukawa couplings

$$\mathcal{L}_y = \sum_{j=1}^{N_f} y_j\bar{\psi}_j\psi_j\phi. \tag{5}$$

Here we take $y_j = y$ so that the set of Fermi fields ψ_j can be regarded as a gauge multiplet, and for $N_f = 3$ the model describes a quark interacting with a scalar field. If the symmetry is broken and the scalar field has a nonvanishing vev, $v = \langle\phi\rangle$, then the Higgs field h is defined by the shift $h = \phi - v$ and the fermion acquires the mass $m = yv$. We refer to m as the top mass even if the present study applies to any fermion with a Yukawa coupling to the scalar field.

Let us follow the method of Ref. [15] and integrate the fermions exactly. The exact action can be written in terms of a shifted Higgs field $h = \phi - \varphi$ where φ is a generic constant shift. The field h becomes the standard Higgs field when $\varphi = v$, but we leave the variable φ unconstrained at this stage. Integrating out the fermions, the bilinear fermionic terms are replaced by an effective action

$$S = \int \mathcal{L}d^4x \rightarrow \int \mathcal{L}_h d^4x + S_{\text{eff}}[h], \tag{6}$$

where

$$\mathcal{L}_h = \frac{1}{2}\partial^\mu h\partial_\mu h + V_c(\varphi + h), \tag{7}$$

and the effective action S_{eff} is given by

$$S_{\text{eff}}[h] = -N_f\,\text{logdet}[G_m^{-1} + yh]_{m=y\varphi}, \tag{8}$$

with the fermionic inverse propagator G_m^{-1} defined as

$$G_m^{-1} = -i\gamma^\mu\partial_\mu + m, \tag{9}$$

and the mass set to the value $m = y\varphi$. These equations are exact and hold for any choice of the variable φ as a consequence of the exact integration of the fermionic fields.

It is obvious that the effective action in Eq. (8) is far too complicated to be treated exactly. From a formal point of view it can be expanded in powers of the field h

$$S_{\rm eff}[h] = -N_f \,{\rm Tr}\log G_m^{-1} - N_f \sum_{n=1}^{\infty} (-1)^{n+1} y^n \,{\rm Tr}\{(G_m \cdot h)^n\}, \tag{10}$$

where the products $G_m \cdot h \cdot G_m \cdot h \cdots$ are nonlocal products of operators with the internal space variables integrated over.

The expansion is convergent if the norm $\|yhG_m\| < 1$. We will show that in the strong coupling limit $y \gg \lambda_B \approx 1$, in units of the cutoff (or of the lattice spacing), the physical range of parameters, where $m \ll 1$, is reached for $0.2 < m_B/y < 0.25$. In fact, in that limit, the one-loop approximation is entirely characterized by the single parameter m_B/y that takes its critical value when $m_B/y = \sqrt{N_f}/(2\pi)$, that is ≈ 0.28 for $N_f = 3$. We will discuss this scaling later, in Sec. IV. In that physical range, provided that we do not reach the critical point, the average $\langle hh \rangle \approx Z/M_R^2$ where $Z \approx 1$, is a wave function renormalization factor and M_R is a renormalized mass of order $M_R \approx m_B$, while in units of the cutoff $\langle G_m G_m \rangle \approx -1/(4\pi^2)$, so that

$$\|yhG_m\|^2 \approx \frac{y^2}{4}\,{\rm Tr}\langle hG_m hG_m \rangle \approx \left(\frac{yZ}{4\pi M_R}\right)^2, \tag{11}$$

and for $Z = 1$, $M_R \approx m_B$ we see that the expansion makes sense provided that

$$\|yhG_m\| \approx 0.08 \cdot \frac{y}{m_B} < 1. \tag{12}$$

In the physical range of parameters where $m_B/y \approx 0.25$ this is never too large, even in the very strong coupling limit.

In fact the expansion in Eq. (10) is not a perturbative expansion in the parameter y but can be regarded as an expansion in terms of the fluctuating field h. Provided that $\langle hh \rangle$ is small, the Gaussian fluctuations are enough and the quartic and higher-order terms can be dropped without affecting the nonperturbative nature of the approximation. This is the case for the Hubbard model of antiferromagnetism in the strong coupling limit [15]. The approximation breaks down at the critical point where the fluctuations of the field h are large and $\langle hh \rangle$ diverges. However the triviality of the scalar theory requires that a finite cutoff is retained, that is to say that the critical point is never reached. In the physical range of the parameters, before the critical point is reached, even in the strong coupling limit the fluctuations are small and we can neglect the higher-order terms in the expansion. This approximation spoils the variational character of the method, but the nonperturbative nature of the approximation is maintained as for RPA approximation that is very similar to the present method from a formal point of view. In principle the approximation can be improved by inclusion of higher-order terms in the expansion, yielding a more complicated set of coupled equations that can be solved by numerical techniques. However the first nonvanishing contribution comes from the quartic term $\langle hhhh \rangle$ that is much smaller than the second-order term in the physical range of the parameters. Its actual value can be evaluated for a more accurate control of the approximation.

The truncated expansion for $S_{\rm eff}$ reads

$$S_{\rm eff}^{(2)}[h] = -N_f \,{\rm Tr}\log G_m^{-1} - yN_f \,{\rm Tr}(G_m \cdot h) + \frac{1}{2} y^2 N_f \,{\rm Tr}(G_m \cdot h \cdot G_m \cdot h), \tag{13}$$

and our starting point is the vacuum-to-vacuum amplitude

$$Z = \int \mathcal{D}_h e^{-[\int \mathcal{L}_h d^4x + S_{\rm eff}^{(2)}[h]]}. \tag{14}$$

Inserting a Gaussian trial functional, the amplitude Z is written as

$$Z = \int \mathcal{D}_h e^{-[\frac{1}{2}\int h(x) g^{-1}(x,y) h(y) d^4x d^4y + S_{\rm int}[h]]}, \tag{15}$$

where $g^{-1}(x, y)$ is a trial inverse propagator, and

$$S_{\rm int}[h] = -\frac{1}{2}\int h(x) g^{-1}(x, y) h(y) d^4x d^4y + \int \mathcal{L}_h d^4x + S_{\rm eff}^{(2)}[h] \tag{16}$$

is regarded as an interaction term. We define the Gaussian average of a generic operator $\mathcal{O}$ according to

$$\langle \mathcal{O} \rangle = \frac{1}{Z_0}\int \mathcal{D}_h \mathcal{O} e^{-\frac{1}{2}\int h(x) g^{-1}(x,y) h(y) d^4x d^4y}, \tag{17}$$

where

$$Z_0 = \int \mathcal{D}_h e^{-\frac{1}{2}\int h(x) g^{-1}(x,y) h(y) d^4x d^4y}. \tag{18}$$

It follows that $\langle h \rangle = 0$ and $\langle h(x) h(y) \rangle = g(x, y)$. Moreover $\langle \phi \rangle = \varphi$ and the variable φ is the expectation value of the scalar field.

By Jensen inequality [16,22] the effective potential $V(\varphi)$ is bounded [11,23] by a Gaussian functional

$$V(\varphi) \le V_{\rm GEP}[g], \tag{19}$$

where the Gaussian functional is defined as

$$V_{\rm GEP}[g] = \langle S_{\rm int} \rangle - \log \int \mathcal{D}_h e^{-\frac{1}{2}\int h(x) g^{-1}(x,y) h(y) d^4x d^4y} \tag{20}$$

and is equivalent to the first-order effective potential in the presence of the interaction term $S_{\rm int}$. The bound in Eq. (19) allows for a variational determination of the trial propagator $g(x, y)$, and the GEP is defined as the minimum of the functional

$$V_{\rm GEP}(\varphi) \equiv V_{\rm GEP}[g_0] \tag{21}$$

with the optimal propagator g_0 satisfying the gap equation

$$\left(\frac{\delta V_{\rm GEP}}{\delta g}\right)_{g_0} = 0. \tag{22}$$

This stationary condition must hold at each point φ and the resulting propagator g_0 depends on the value of φ.

A trivial calculation yields

$$V_{\mathrm{GEP}}[g] = V_c(\varphi) + V_{1L}(\varphi) + V_0[g] + V_2[g] + V_F[g]. \tag{23}$$

The first two terms are the classical potential and the one-loop term and do not depend on the trial propagator since

$$V_{1L}(\varphi) = N_f(\mathrm{Tr}\log G_m)_{m=y\varphi}. \tag{24}$$

The third term has no explicit dependence on φ

$$V_0[g] = I_1[g] + \frac{\lambda_B}{8} I_0^2[g] + \frac{1}{2}\int \frac{d^4p}{(2\pi)^4}\left[\frac{g(p)}{g_B(p)} - 1\right]. \tag{25}$$

Here $g(p)$ is the Fourier transform of $g(x, y)$, the bare propagator is $g_B^{-1} = m_B^2 + p^2$, and the integrals I_0, I_1 are defined as

$$I_1[g] = -\frac{1}{2}\int \frac{d^4p}{(2\pi)^4}\log g(p), \tag{26}$$

$$I_0[g] = \int \frac{d^4p}{(2\pi)^4} g(p). \tag{27}$$

All the integrals in the four-dimensional Euclidean space are made finite by insertion of a cutoff Λ, and taking $p^2 < \Lambda^2$. The fourth term $V_2[g]$ has a quadratic explicit dependence on φ

$$V_2[g] = \frac{\lambda_B}{4}\varphi^2 I_0[g], \tag{28}$$

and the last term $V_F[g]$ follows from the fermionic loop in the average of the quadratic part of Eq. (13)

$$V_F[g] = \frac{y^2 N_f}{2}\int \frac{d^4p}{(2\pi)^4} K(p)g(p), \tag{29}$$

where the kernel $K(p)$ is the one-loop fermion polarization function

$$K(p) = \int \frac{d^4q}{(2\pi)^4}\,\mathrm{Tr}\{G_m(p+q)G_m(q)\}_{m=y\varphi}, \tag{30}$$

and $G_m(p)$ follows by Fourier transform of Eq. (9)

$$G_m(p) = (-\gamma_\mu p^\mu + m)^{-1} = \frac{\gamma_\mu p^\mu + m}{p^2 + m^2}. \tag{31}$$

Exact and approximate expressions for the kernel $K(p)$ are reported in Appendix A.

According to Eq. (22), the functional derivative of Eq. (23) gives a gap equation that reads

$$g_0^{-1} = p^2 + \Omega^2[g_0] + N_f y^2 K(p), \tag{32}$$

where the mass functional $\Omega^2[g]$ is defined as

$$\Omega^2[g] = m_B^2 + \frac{1}{2}\lambda_B\varphi^2 + \frac{1}{2}\lambda_B I_0[g] \tag{33}$$

and does not depend on p, while $K(p)$ does not depend on g. In the limit $y \to 0$ the optimal trial propagator takes the simple form $g_0^{-1} = g_\Omega^{-1} = p^2 + \Omega^2$ where the mass parameter $\Omega^2 \equiv \Omega^2[g_0]$ is the self-consistent solution of Eq. (33). In this limit there is no wave function renormalization and we recover the GEP for a scalar theory

$$V_{\mathrm{GEP}}(\varphi) = V_c(\varphi) + V_0[g_\Omega] + V_2[g_\Omega], \tag{34}$$

where the last two terms have an implicit dependence on φ through g_Ω. This case has been studied in Ref. [12] in some detail.

In general the propagator g_0 has a more complicated dependence on p as a consequence of the Yukawa interaction that adds the last term in Eq. (32). We can study this dependence in some detail in the limit $p \to 0$. In this limit the kernel $K(p)$ is an analytic function of p^2 and can be expanded in powers yielding

$$K(p) \approx a_0(m) + a_1(m)p^2 + \mathcal{O}(p^4), \tag{35}$$

where the functions $a_i(m)$ are derived in Appendix A and must be evaluated for $m = y\varphi$. The optimal propagator in Eq. (32) can then be written in the same limit as

$$g_0(p) \approx \frac{Z}{p^2 + M_R^2}, \tag{36}$$

where the wave function renormalization constant reads

$$Z^{-1} = 1 + y^2 N_f a_1(m), \tag{37}$$

and the renormalized mass is

$$M_R^2 = Z[\Omega^2 + y^2 N_f a_0(m)]. \tag{38}$$

It is instructive to explore the content of the approximation in terms of graphs. The solution g_0 of the gap equation (32) can be regarded as the solution of the Dyson equation

$$g(p) = g_\Omega(p) + g(p)\cdot[-y^2 N_f K(p)]\cdot g_\Omega(p), \tag{39}$$

which sums up the whole class of ring diagrams. From a formal point of view this kind of approximation is equivalent to RPA, but here the self-consistent parameter $\Omega^2 = \Omega^2[g_0]$ and the corresponding propagator $g_\Omega^{-1} = p^2 + \Omega^2$ are functions of φ while in RPA they are fixed at their mean-field value. Thus the dependence of the effective potential on φ is different, as are the predictions for the vev.

Inserting back Eq. (32) in Eq. (23) the effective potential takes the simple form

$$V_{\mathrm{GEP}}(\varphi) = V_c(\varphi) + V_{1L}(\varphi) + \left[I_1 - \frac{1}{8}\lambda_B I_0^2\right], \tag{40}$$

where we recognize the classic term, the one-loop correction, and the standard GEP term of a scalar theory [11,12]

(in brackets). However, here the integrals I_0, I_1 are evaluated for $g = g_0$, which is a solution of the interacting gap equation (32); thus, the last term does depend on the coupling y and gives rise to large deviations from the simple one-loop result in the strong coupling limit.

The numerical evaluation of the effective potential can be obtained more easily by a simple integration of the first derivative

$$\frac{dV_{\mathrm{GEP}}}{d\varphi} = \frac{\partial V_{\mathrm{GEP}}}{\partial \varphi} + \int \left(\frac{\delta V_{\mathrm{GEP}}}{\delta g}\right)\left(\frac{dg}{d\varphi}\right)\frac{d^4p}{(2\pi)^4}, \tag{41}$$

which by insertion of Eq. (22) is equivalent to the partial derivative

$$\frac{dV_{\mathrm{GEP}}(\varphi)}{d\varphi} = \frac{\partial V_{\mathrm{GEP}}(\varphi)}{\partial \varphi} \tag{42}$$

yielding

$$\frac{dV_{\mathrm{GEP}}}{d\varphi} = \left[m_B^2\varphi + \frac{\lambda_B}{3!}\varphi^3 + \frac{dV_{1L}}{d\varphi}\right] + \frac{\lambda_B}{2} I_0 \varphi + \frac{y^2 N_f}{2}\int \frac{d^4p}{(2\pi)^4}\frac{dK(p)}{d\varphi} g(p). \tag{43}$$

Here the trial propagator must be set to its optimal value g_0 for any φ point, yielding an implicit dependence on that variable. Explicit expressions for the derivatives of $K(p)$ and V_{1L} are reported in Appendices B and C, respectively.

III. COMPARISON WITH LATTICE DATA

For any set of Lagrangian parameters the GEP can be obtained by solving the gap equation (32) and integrating the derivative in Eq. (43). In order to compare with lattice data some care must be taken in the choice of the energy units. While we would prefer units of the cutoff Λ, lattice data are usually reported in units of the lattice spacing a. Actually the cutoff can be thought of as defining an effective lattice spacing $a = c/\Lambda$, with an unknown constant scale factor $c = a\Lambda$ of order unity that depends on the approximation scheme and can be determined by a direct comparison with the lattice data. Once the constant scale factor is fixed, the predictions of the GEP can be compared with the lattice data [12]. Some lattice data on the Higgs-top model are discussed in Ref. [21]. For a comparison we use the same set of parameters: $y = 0.5$, $\lambda_B = 0.1$, and $m_B^2 = 0.1$. As in other lattice calculations, they take a large even number of fermions because of a well-known duplication problem. We use the same value $N_f = 8$ in this section. The scale factor has been determined as $c = 2.34$ by a fit of the vev as shown in Fig. 1. Here the vev is defined as the minimum point of the GEP and is reported in units of Λ/c in order to fit the lattice data.

With the scale factor fixed, the derivative of the effective potential is evaluated by Eq. (43) and reported in Fig. 2 for the parameter set $\lambda_B = 0.1$, $y = 0.5$, $m_B^2 = 0.1$, $N_f = 8$ in units of the effective lattice spacing $a = c/\Lambda$. The lattice data of Ref. [21] are shown in the same figure for comparison. We find a good general agreement, with no need for any other tuning of the parameters. Unfortunately, we only found detailed lattice data for comparison in this weak coupling limit where the variational method does not add too much to the usual perturbative treatment of the model. Some recent lattice data have been reported in the strong coupling limit but for the special limit cases $\lambda_B \to \infty$ and $\lambda_B = 0$ [24]. Strong coupling deviations from the one-loop predictions will be discussed in the next section.

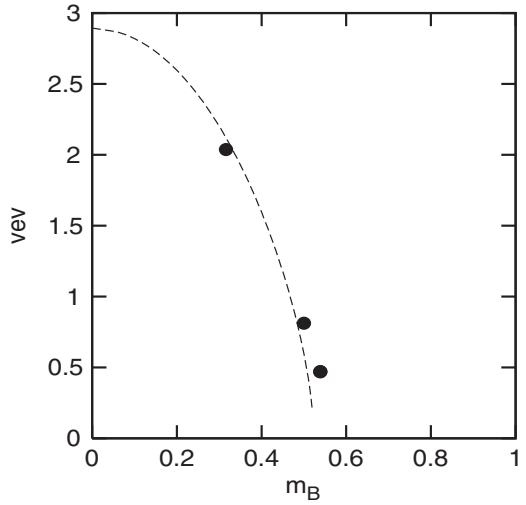

FIG. 1. The vev as a function of the bare mass m_B in units of Λ/c for $\lambda_B = 0.1$, $y = 0.5$, and for a scale factor $c = 2.34$ (dashed line). With that choice of scale the GEP interpolates the lattice data of Ref. [21] (circles).

However, even in this weak coupling limit, at variance with the perturbative method that predicts an unstable

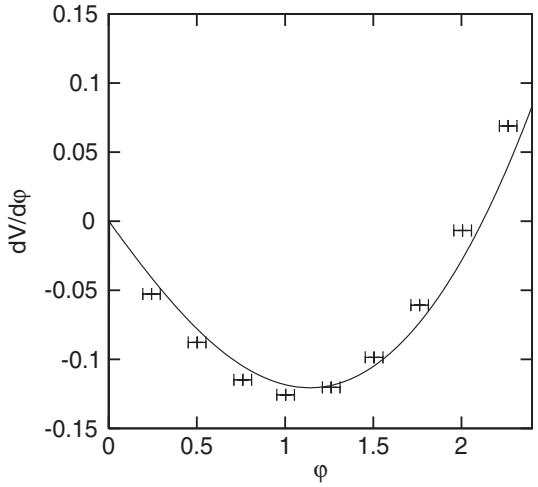

FIG. 2. The derivative of the effective potential $dV/d\varphi$ is reported as a function of the variable φ in units of Λ/c with $c = 2.34$, and for the parameter set $\lambda_B = 0.1$, $y = 0.5$, $m_B^2 = 0.1$, $N_f = 8$. The GEP (solid line) is compared with the lattice data points of Ref. [21] (error bars).

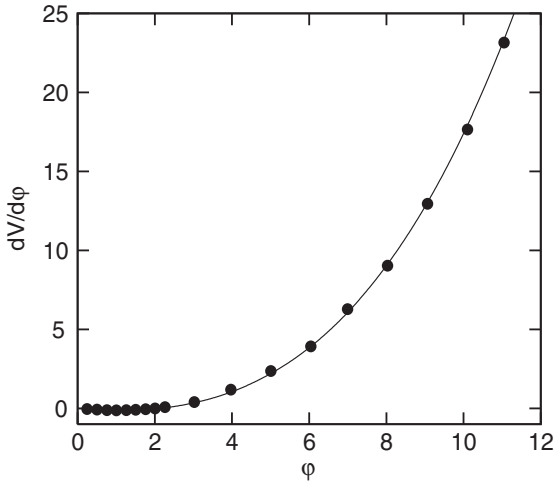

FIG. 3. The derivative of the effective potential $dV/d\varphi$ is reported as a function of the variable φ in units of Λ/c with $c = 2.34$, and for the same parameter set as for Fig. 2, but for a wide range of φ. The GEP (solid line) is compared with the lattice data points of Ref. [21] (circles). The derivative is positive for large values of φ, even when $\varphi > \Lambda$, and no vacuum instability occurs in the GEP.

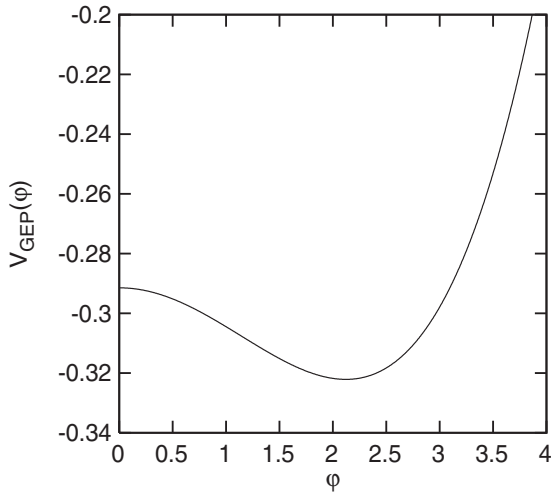

FIG. 4. The GEP $V_{\mathrm{GEP}}(\varphi)$ is shown as a function of the variable φ in units of the effective lattice spacing $a = c/\Lambda$ with $c = 2.34$, and for the same parameter set as for Fig. 2.

vacuum for large values of φ, the GEP is perfectly bounded and predicts a stable vacuum as shown in Fig. 3 in agreement with the lattice calculations, confirming that the instability of the vacuum is not a consequence of the interaction with the fermions but a misleading internal problem of the standard perturbative approximation, emerging when the field is much larger than the cutoff [21]. Actually, vacuum instability emerges in the renormalized perturbation theory because the renormalized couplings are allowed to assume any value, whereas in bare theories, like the present variational method or lattice calculations, only a limited range of renormalized couplings are possible, which vanish logarithmically with the cutoff. By inspection of Eq. (43) we observe that in the unphysical limit of $\varphi \gg \Lambda$ the integrals become irrelevant as they are cut at a relatively small value of Λ. The negative unstabilizing one-loop term vanishes as $\sim 1/\varphi$ in that limit according to Eq. (C3), and the leading term in Eq. (43) is the positive classic φ^3 term. Thus the effective potential cannot be unbounded for large values of the field.

For the same set of parameters the GEP is reported in Fig. 4 in units of the effective lattice spacing. The minimum is at $\varphi = v \approx 2.1$ and in the same units the top mass is $m = yv \approx 1$. It is remarkable that the breaking of symmetry is entirely driven by the Yukawa interaction with the fermions: here $m_B^2 > 0$, the classical potential is symmetric and would predict a vanishing vev. Thus in the SM the symmetry is broken because of the large Yukawa coupling of the top quark $y \approx 0.7$ that gives rise to a finite vev and gives back a mass to all the fermions. There is no need for unphysical negative bare squared masses $m_B^2 < 0$ in the Lagrangian, which are quite difficult to be explained for a free field theory. Moreover, in several extensions of the SM the Higgs sector can be quite simplified, because there is no need to assume that the classical potential has a minimum at a broken symmetry point $\varphi \neq 0$. For instance, the minimal left-right symmetric extension of the SM [25,26] does not require the existence of scalar bidoublet fields, and a model with only two doublets is perfectly viable [27,28].

IV. STRONG COUPLING LIMIT

The GEP has already been studied for large values of the self-coupling λ_B of the scalar field in the past [12]. The method has been shown to be reliable for large couplings, even if these are almost ruled out by the recent experimental evidence of a light Higgs mass. In this section we would like to explore the limit of a strong Yukawa coupling, much larger than λ_B. We take $\lambda_B = 0.1$ and $N_f = 3$ in order to represent a QCD quark multiplet like the top quark. Moreover, we use units of Λ in this section ($c = 1$) and explore the model for a large coupling y and generic values of the bare mass. Thus, in these units we are left with two free parameters, y and m_B^2. However, the physical requirement of a nonvanishing small top mass, quite smaller than the cutoff ($m \ll 1$ in our units), decreases our degree of freedom and limits the ratio of the free parameters in the range $0.2 < m_B/y < 0.25$. In fact, the physical masses can be regarded as the inverse of correlation lengths $\xi = 1/m$, and the condition $m \ll 1$ is equivalent to the requirement that ξ is much larger than the effective lattice spacing. Only in that limit does the model make sense. Actually, we can show that the predictions of the one-loop approximation only depend on the single parameter y/m_B in the strong coupling limit $y \gg \lambda_B \approx 1$. When the physical top mass $m = yv$ is displayed as a function of m_B/y, the one-loop

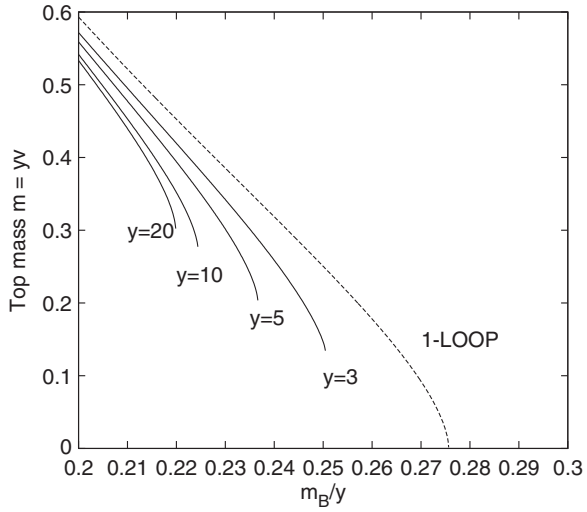

FIG. 5. The top mass as a function of the parameter (m_B/y), for a range of Yukawa couplings going from $y = 3$ to $y = 20$, according to the GEP. Energies are in units of the cutoff Λ. The one-loop data collapse on a single curve (dashed line).

data collapse on a single curve in the strong coupling limit and do not depend on y as displayed in Fig. 5.

Evidence for this strong coupling scaling can be found by a simple analysis of the single terms contributing to the effective potential. By taking the mass $m = y\varphi$ as an independent variable, the derivative of the effective potential follows from Eq. (43)

$$\frac{1}{m}\frac{dV_{\mathrm{GEP}}}{dm} = \left[2\left(\frac{dV_{1L}}{dm^2}\right) + \left(\frac{m_B}{y}\right)^2 + \frac{\lambda_B}{3!y^4}m^3\right] + \frac{\lambda_B}{2y}I_0 + y^2 N_f \int \frac{d^4p}{(2\pi)^4}\frac{dK(p)}{dm^2}g(p). \tag{44}$$

We recognize a first term in square brackets arising from the classical plus one-loop potential, a second term of order $\sim\lambda_B/y$ arising from the standard GEP correction to the scalar potential, and a third term of order $\sim y^2$ arising from our nonperturbative treatment of the Yukawa interaction. We observe that V_{1L} and K have no explicit dependence on y and m_B when written as functions of the variable m. Thus at one-loop, in the strong coupling limit $y \gg \lambda_B$, the derivative of the effective potential reads

$$\frac{dV}{dm} = m\left[2\left(\frac{dV_{1L}}{dm^2}\right) + \left(\frac{m_B}{y}\right)^2\right] \tag{45}$$

and only depends on the ratio m_B/y. The stationary points of the potential are the solution of the equation $dV/dm = 0$. When the symmetry is broken we find a maximum at $m = 0$ and a minimum given by the solution of the equation

$$\left(\frac{dV_{1L}}{dm^2}\right) = -\frac{1}{2}\left(\frac{m_B}{y}\right)^2, \tag{46}$$

thus a plot of the one-loop top mass m at the minimum, as a function of the single parameter (m_B/y) must follow a single curve for any strong coupling y.

This single curve predicts a universal critical point $(m_B/y)_c$ for the single parameter, when the maximum and minimum coincide:

$$\left(\frac{dV_{1L}}{dm^2}\right)_{m=0} = -\frac{1}{2}\left(\frac{m_B}{y}\right)^2, \tag{47}$$

and from the explicit expression in Eq. (C3) we obtain

$$\left(\frac{m_B}{y}\right)_c = \frac{\sqrt{N_f}}{2\pi}, \tag{48}$$

which for $N_f = 3$ is $(m_B/y)_c \approx 0.276$. In this strong coupling regime, deviations from the single parameter scaling can only arise from the nonperturbative last term in Eq. (44). Thus deviations from scaling can be used as a measure of the nonperturbative effects in the GEP. The top mass m, as emerging from the GEP calculation, is reported in Fig. 5 as a function of the scaling parameter m_B/y for several values of the Yukawa coupling ranging from $y = 3$ to $y = 20$. All the one-loop data collapse on the dashed line. Deviations from the scaling are present when the GEP is considered, but they are small for the phenomenological value $y \approx 0.7$. These deviations cannot be neglected in the range of large couplings. In Fig. 6 the top mass is reported as a function of the Yukawa coupling y for a typical value of the parameter $m_B/y = 0.21$. We notice the different behavior of one-loop and GEP approximations: the top mass is reduced by fluctuations. Moreover, the fluctuations give rise to a decreasing of the wave function renormalization constant Z according to Eq. (37) as shown in Fig. 7.

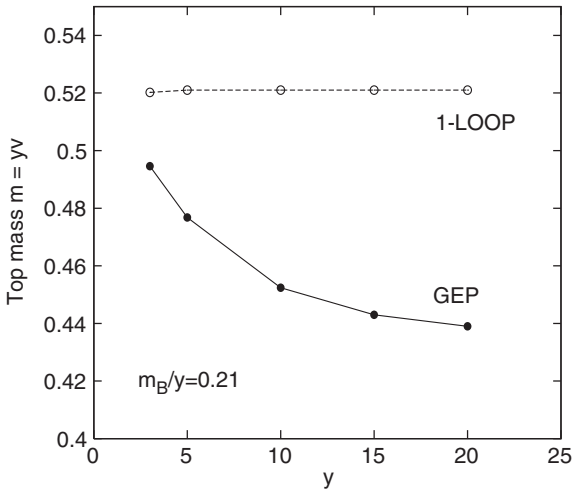

FIG. 6. The top mass as a function of the Yukawa coupling y, for a typical value of the parameter $(m_B/y) = 0.21$. The prediction of the GEP (solid circles) is compared with the steady one-loop data (open circles). Masses are in units of the cutoff.

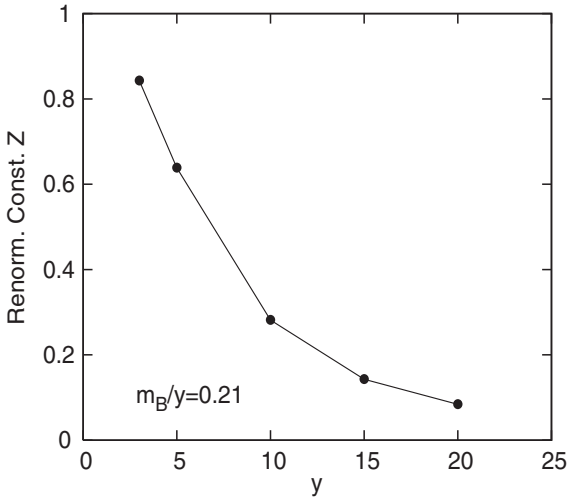

FIG. 7. The wave function renormalization constant Z is reported according to Eq. (37) as a function of the Yukawa coupling, for a typical value of the parameter $(m_B/y) = 0.21$.

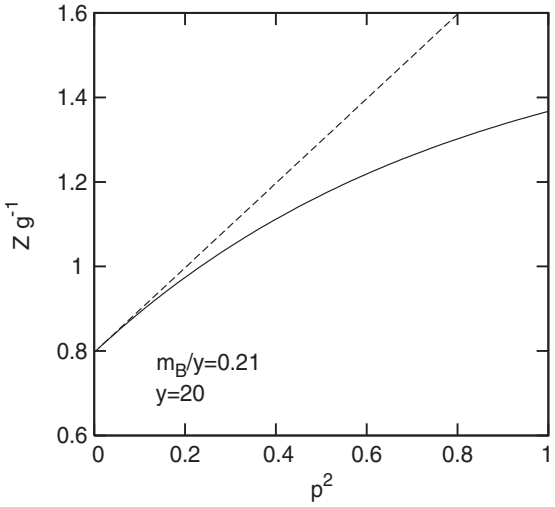

FIG. 9. The same as Fig. 8 but for a strong Yukawa coupling $y = 20$ (solid line). The linear approximate inverse propagator is shown for comparison (dashed line).

This effect is negligible for weak couplings but becomes very large in the strong coupling limit.

More insights come from a closer study of the Higgs propagator $g_0(p)$ that solves Eq. (32). The renormalized inverse propagator Zg_0^{-1} is reported as function of p^2 for a typical value of the parameter $m_B/y = 0.21$ in Figs. 8 and 9. The approximate linear expression in Eq. (36), derived for small values of p, is shown for comparison. In Fig. 8, for a moderately large Yukawa coupling $y = 3$, deviations from linearity are small and only occur for very large values of p^2. Deviations are large in the strong coupling limit, as shown in Fig. 9 for $y = 20$.

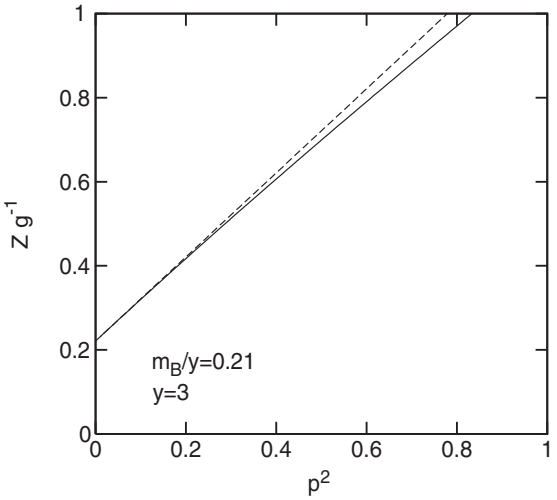

FIG. 8. The renormalized inverse propagator Zg^{-1} is shown as a function of p^2, in units of the cutoff Λ, for a typical value of the parameter $(m_B/y) = 0.21$, and for a moderate coupling $y = 3$ (solid line). Here g is the optimal propagator solving Eq. (32). The linear approximate inverse propagator of Eq. (36) is shown for comparison (dashed line).

A shortcoming of the approximation comes from the breakdown of the convergence criterion when approaching the critical point. Before reaching the critical point, the fluctuations of the Higgs field become large enough to make the expansion in Eq. (10) useless. In fact, in Fig. 5 the plots do not reach the critical point, but we checked that the criterion of convergence is satisfied for the reported data. From a technical point of view, the renormalized mass in Eq. (38) becomes small when approaching the critical point, and it vanishes before reaching the transition. A real pole occurs in the Higgs propagator and the integrals diverge. However, this is just a sign that the Higgs fluctuations are too large and the expansion in Eq. (10) does not hold any more. In our calculation we never let the renormalized mass be too small, in order to fulfill the convergence criterion. Thus our data are still reliable even if they cannot span the entire range of the free parameters.

V. CONCLUSIONS

We have studied the Higgs-top model by a nonperturbative variational extension of the GEP that incorporates fermions. While the pure GEP is known to give trivial results for the fermions [20], some effects of their fluctuations have been included in the GEP by an hybrid method: fermions are integrated out exactly and the resulting effective action is expanded in powers of the fluctuating Higgs field. Even in the strong coupling limit, a second-order expansion provides reliable predictions for a large range of the free parameters. By fixing an effective lattice spacing, the GEP is found in good general agreement with the available lattice data for the model.

In the strong coupling limit the Gaussian fluctuations reduce the vev and the top mass, as displayed by a comparison with the one-loop approximation. In this limit the

one-loop data are seen to follow a single-parameter scaling, while the Gaussian fluctuations give rise to important deviations from scaling.

At variance with renormalized perturbation theory, this study confirms that the Higgs-top model has a perfectly stable vacuum even in the strong coupling limit and that, in the presence of Yukawa couplings with fermions, there is no need for a finite vev in the classical potential. In fact, a nonvanishing vev can be predicted even when $m_B^2 > 0$ and the classical potential has no broken symmetry vacuum. Thus fluctuations are very relevant for determining the correct vev, and naive discussions based on the classical potential cannot be used for the Higgs-top model.

On general grounds, inclusion of fermions in a nonperturbative and almost analytical calculation is of interest by itself. Moreover the same method could be used in the framework of effective theories [29] or in a low-energy study of gauge theories like QCD when the perturbative approximation breaks down. While the GEP was derived for the SU(2) gauge theory in the past [16], no previous attempt has been reported for incorporating fermions. Thus the present study could be extended in that direction.

APPENDIX A: POLARIZATION FUNCTION $K(p)$

The fermionic polarization function $K(p)$ has been calculated exactly, integrating inside the hypersphere $p^2 < \Lambda^2$ in the four-dimensional Euclidean space. Inserting Eq. (31) into Eq. (30) and evaluating the trace,

$$K(p) = 4\int_\Lambda \frac{d^4q}{(2\pi)^4}\frac{m^2 - q^2 - q\cdot p}{(m^2+q^2)(m^2+q^2+p^2+2q\cdot p)}. \tag{A1}$$

Here the Feynman trick cannot be used because of the finite cutoff. However, by a tedious but straightforward calculation the exact polarization function can be written as

$$K(p) = K_0 + K_1(p) + K_2(p) + K_3(p), \tag{A2}$$

where K_0 is the constant

$$K_0 = -\frac{1}{8\pi^2}\left[\Lambda^2 - m^2\log\frac{\Lambda^2+m^2}{m^2}\right], \tag{A3}$$

and the three functions $K_i(p)$ follow

$$K_1(p) = \frac{4m^2+p^2}{16\pi^2}\log\frac{\Lambda^2+m^2}{m^2} + \frac{\Lambda^2}{32\pi^2p^2}(6m^2-\Lambda^2), \tag{A4}$$

$$K_2(p) = \frac{\beta\delta + p^4 - m^4}{32\pi^2p^2} + \frac{m^2}{8\pi^2}\log\frac{\beta+\delta}{2m^2}, \tag{A5}$$

$$K_3(p) = -\frac{4m^2+p^2}{16\pi^2p^2}J(p), \tag{A6}$$

where β and δ are the functions

$$\beta(p) = m^2 + \Lambda^2 - p^2, \tag{A7}$$

$$\delta(p) = \sqrt{\beta^2 + 4m^2p^2}, \tag{A8}$$

and J is the integral

$$J(p) = \int_{m^2}^{m^2+\Lambda^2}\frac{dx}{x}\sqrt{(x-p^2)^2+4m^2p^2}. \tag{A9}$$

The integral J has been evaluated in Ref. [12] and its explicit expression is

$$J(p) = \frac{\beta+\delta-2m^2}{2} - p^2\rho, \tag{A10}$$

where ρ is the function

$$\rho(p) = \log\left|\frac{t_2}{t_1}\right| - \frac{m}{p}\left(\frac{1}{t_2}-\frac{1}{t_1}\right) + \sqrt{1+\frac{4m^2}{p^2}}\log\left|\frac{(t_2-t_-)(t_1-t_+)}{(t_2-t_+)(t_1-t_-)}\right|, \tag{A11}$$

and its arguments are

$$t_\pm = -\frac{p}{2m} \pm \sqrt{1+\frac{p^2}{4m^2}}, \tag{A12}$$

$$t_1 = \frac{m}{p}; \qquad t_2 = \frac{\beta+\delta}{2mp}. \tag{A13}$$

It can be easily seen that the singular terms cancel in Eq. (A2) and the resulting function $K(p)$ is an analytic function of p^2. Its expansion in powers of p^2 reads

$$K(p) = \sum_{n=0}^{\infty} a_n(m)p^{2n}, \tag{A14}$$

where the coefficients $a_n(m)$ are functions of m^2. In units of the cutoff Λ the first two coefficients of the expansion are

$$a_0(m) = -\frac{1}{4\pi^2}\left[1 + \frac{2m^2}{1+m^2} - 3m^2\log\frac{1+m^2}{m^2}\right], \tag{A15}$$

$$a_1(m) = \frac{1}{8\pi^2}\log\frac{1+m^2}{m^2} - \frac{(6m^4+21m^2+7)}{48\pi^2(1+m^2)^3}. \tag{A16}$$

APPENDIX B: DERIVATIVE OF $K(p)$

Explicit expressions for the exact and approximate polarization function $K(p)$ have been reported in Appendix A. The derivative can be written as

$$\frac{dK(p)}{d\varphi} = 2ym\frac{dK(p)}{dm^2}, \tag{B1}$$

where

$$\frac{dK(p)}{dm^2} = \frac{dK_0}{dm^2} + \frac{dK_1(p)}{dm^2} + \frac{dK_2(p)}{dm^2} + \frac{dK_3(p)}{dm^2}, \tag{B2}$$

and the single terms K_i are given in Appendix A. By an explicit calculation we obtain

$$\frac{dK_0}{dm^2} = -\frac{1}{8\pi^2}\left[\frac{\Lambda^2}{\Lambda^2+m^2} - \log\frac{\Lambda^2+m^2}{m^2}\right], \tag{B3}$$

$$\frac{dK_1(p)}{dm^2} = \frac{1}{4\pi^2}\left[\log\frac{\Lambda^2+m^2}{m^2} - \frac{\Lambda^2}{\Lambda^2+m^2}\right] + -\frac{\Lambda^2p^2}{16\pi^2m^2(\Lambda^2+m^2)} + \frac{3\Lambda^2}{16\pi^2p^2}, \tag{B4}$$

$$\frac{dK_2(p)}{dm^2} = -\frac{1}{8\pi^2} - \frac{m^2}{16\pi^2p^2} + \frac{(\Lambda^2+m^2)^2}{16\pi^2p^2\delta} + \frac{m^2-\Lambda^2}{16\pi^2\delta} + \frac{1}{8\pi^2}\log\frac{\beta+\delta}{2m^2} + \frac{m^2}{8\pi^2\delta}\left[1+\frac{2p^2}{\beta+\delta}\right], \tag{B5}$$

$$\frac{dK_3(p)}{dm^2} = -\frac{(4m^2+p^2)}{16\pi^2p^2}\frac{dJ(p)}{dm^2} - \frac{J(p)}{4\pi^2p^2}, \tag{B6}$$

where the functions β, δ, and J are defined in Appendix A. The derivative of J follows as

$$\frac{dJ(p)}{dm^2} = \frac{\beta+2p^2-\delta}{2\delta} - \frac{2p^2(\Lambda^2+2m^2)}{m^2(\Lambda^2+m^2)} + p^2\frac{\beta+2m^2+\delta}{\beta+\delta} \times\left[\frac{1}{m^2} - \frac{\beta+2p^2+\delta}{\delta(\beta+\delta)}\right] - \frac{2p}{\sqrt{p^2+4m^2}} \times\log\left|\frac{(t_2-t_-)(t_1-t_+)}{(t_2-t_+)(t_1-t_-)}\right| \times\left|+\frac{p^2[(\beta+2p^2)(4m^2+p^2)+(4m^2-p^2)\delta]}{(m^2+\Lambda^2)(\beta+\delta)\delta}\right|, \tag{B7}$$

where the functions $t_\pm$, t_1, t_2 are defined in Appendix A.

APPENDIX C: ONE-LOOP POTENTIAL V_{1L} AND ITS DERIVATIVE

The one-loop term $V_{1L}(\varphi)$ is defined in Eq. (24) and its explicit evaluation, in terms of $m = y\varphi$, yields the integral

$$V_{1L}(m) = -2N_f\int_0^\Lambda \frac{2\pi^2p^3dp}{(2\pi)^4}\log(m^2+p^2), \tag{C1}$$

and in units of the cutoff Λ

$$V_{1L}(m) = \frac{N_f}{32\pi^2}[1-2\log(1+m^2)] - \frac{N_fm^2}{16\pi^2} + \frac{N_fm^4}{16\pi^2}\log\frac{1+m^2}{m^2}. \tag{C2}$$

The derivative follows

$$\frac{dV_{1L}}{dm^2} = \frac{N_fm^2}{8\pi^2}\log\frac{1+m^2}{m^2} - \frac{N_f}{8\pi^2}, \tag{C3}$$

so that

$$\left(\frac{dV_{1L}}{dm^2}\right)_{m=0} = -\frac{N_f}{8\pi^2}. \tag{C4}$$

[1] R. Gupta, arXiv:hep-lat/9807028.
[2] D. N. Petcher, arXiv:hep-lat/9301015v1.
[3] U.-J. Wiese, "*Foundations and New Methods in Theoretical Physics*," Summer School for Graduate Students, 2009 (unpublished).
[4] R. V. Gavai, Pramana **61**, 889 (2003).
[5] R. V. Gavai, Pramana **67**, 885 (2006).
[6] T. Onogi, Int. J. Mod. Phys. A **24**, 4607 (2009).
[7] S. Chandrasekharan and U.-J. Wiese, Prog. Part. Nucl. Phys. **53**, 373 (2004).
[8] L. I. Schiff, Phys. Rev. **130**, 458 (1963).
[9] G. Rosen, Phys. Rev. **172**, 1632 (1968).
[10] T. Barnes and G. I. Ghandour, Phys. Rev. D **22**, 924 (1980).
[11] P. M. Stevenson, Phys. Rev. D **32**, 1389 (1985).
[12] F. Siringo and L. Marotta, Int. J. Mod. Phys. A **25**, 5865 (2010).
[13] M. Camarda, G. G. N. Angilella, R. Pucci, and F. Siringo, Eur. Phys. J. B **33**, 273 (2003).
[14] L. Marotta, M. Camarda, G. G. N. Angilella, and F. Siringo, Phys. Rev. B **73**, 104517 (2006).
[15] L. Marotta and F. Siringo, Mod. Phys. Lett. B **26**, 1250130 (2012).
[16] F. Siringo and L. Marotta, Phys. Rev. D **78**, 016003 (2008).
[17] F. Siringo, Phys. Rev. D **62**, 116009 (2000).
[18] F. Siringo, Europhys. Lett. **59**, 820 (2002).
[19] L. Marotta and F. Siringo, Eur. Phys. J. C **44**, 293 (2005).
[20] I. Stancu, Phys. Rev. D **43**, 1283 (1991).

[21] Z. Fodor, K. Holland, J. Kuti, D. Nogradi, and C. Schroeder, Proc. Sci., LAT2007 (2007) 056 [arXiv:0710.3151v1].
[22] R. Ibañez-Meier, I. Stancu, and P. M. Stevenson, Z. Phys. C **70**, 307 (1996).
[23] I. Stancu and P. M. Stevenson, Phys. Rev. D **42**, 2710 (1990).
[24] J. Bulava, P. Gerhold, G. W.-S. Hou, K. Jansen, B. Knippschild, C.-J. David Lin, K.-I. Nagai, A. Nagy, K. Ogawa, and B. Smigielski, Proc. Sci., Lattice2011 (2011) 075 [arXiv:1111.4544].
[25] F. Siringo, Eur. Phys. J. C **32**, 555 (2004).
[26] F. Siringo, Phys. Rev. Lett. **92**, 119101 (2004).
[27] F. Siringo and L. Marotta, Phys. Rev. D **74**, 115001 (2006).
[28] F. Siringo, arXiv:1208.3599.
[29] F. Siringo and G. Buccheri, Phys. Rev. D **86**, 053013 (2012).